Int J Clin Exp Med 2016;9(2):1986-1996
www.ijcem.com /ISSN:1940-5901/IJCEM0017754

Original Article

The correlation between ventricular remodeling and arrhythmia in rat with myocardial infarction

Dongmei Zhang[1*], Songbo Chai[2*], Meng Chen[3], Aiming Wu[1], Lixia Lou[1], Mingjing Zhao[1], Yonghong Gao[1], Limin Chai[1], Xiying Lv[1], Yikun Sun[1], Shuoren Wang[1]

[1]Key Laboratory of Chinese Internal Medicine (Beijing University of Chinese Medicine), Ministry of Education, Dongzhimen Hospital, Beijing University of Chinese Medicine, Beijing 100700, China; [2]Department of Cardiology, Henan Province Hospital of TCM, Zhengzhou 450011, Henan, China; [3]School of Preclinical Medicine, Beijing University of Chinese Medicine, Beijing 100029, China. [*]Equal contributors.

Received October 13, 2015; Accepted January 27, 2016; Epub February 15, 2016; Published February 29, 2016

Abstract: Fatal arrhythmias are the major causes of death after acute myocardial infarction (AMI). This study aimed to assess the association of ventricular remodeling and arrhythmia after myocardial infarction. Twelve rats were divided into model and sham groups (n=6). The model group animals were submitted to AMI by left anterior descending coronary artery ligation. Sham operated animals wore wires without ligation. Echocardiography was used to assess cardiac structure and function after 8 weeks. Ventricular fibrillation was induced by electrical stimulation *in vivo*, and partial electrophysiological parameters were detected. In addition, myocardial tissue collagen expression was detected by improved Masson staining and immunohistochemistry. To determine the relationship between cardiac structure/pathology and heart physiological function, multiple linear regression was performed. Compared with sham rats, interventricular septal end diastole and systole (IVSd and IVSs), type III/I collagen ratios, ejection fraction (EF) and ventricular fibrillation threshold (VFT) values were reduced in the model group, while left ventricular diastolic and systolic dimension (LVDd and LVDs), total myocardial collagen, type I and III collagen contents significantly increased. In addition, left and right ventricular effective refractory period to the action potential duration at 90% repolarization level (ERP/APD_{90}) ratios decreased significantly. Interestingly, a linear relationship was obtained between cardiac electrophysiological parameters and cardiac structure as well as myocardial tissue fibrosis. These findings indicate that prevention and treatment of ventricular remodeling is very important in reducing arrhythmia after myocardial infarction.

Keywords: Ventricular remodeling, myocardial fibrosis, arrhythmia, acute myocardial infarction, cardiac electrophysiological

Introduction

The normal heart has structural and electrophysiological heterogeneity [1], which becomes the main cause of ventricular arrhythmia in pathological conditions such as heart failure and myocardial infarction [2]. Ventricular remodeling subsequent to myocardial infarction continuously influences the ventricular systolic function and electrical activity [3]. After acute myocardial infarction (AMI), various fatal arrhythmias (especially ventricular fibrillation) are major causes of death in patients. Arrhythmia is an external manifestation of cardiac electrophysiological changes after myocardial infarction [4]. Indeed, patients with AMI have different degrees and types of arrhythmia, which is common in individuals with ventricular premature beat, ventricular tachycardia and ventricular fibrillation; such patients show ventricular remodeling characteristics, including left ventricular dilatation, fibrosis of infarction areas, myocardial hypertrophy of non-infarction areas, and declined cardiac systolic and diastolic functions after AMI [5]. Low ejection fraction and life-threatening ventricular arrhythmia in patients have been shown to be associated with left ventricular remodeling, rather than left ventricular dysfunction [6]. The relationship between arrhythmia and ventricular remodeling has attracted increasing attention from widening circles of clinicians. Studies have demon-

strated that changes in left ventricular size, left ventricular myocardial area (LVMA), and function over time can be used to predict ventricular arrhythmias after infarction [4].

According to the philosophical principle that the material structure decides its function, it is plausible that changes of cardiac electrophysiological properties reflect those of ion channels in the myocardial cell membrane [7, 8]. Indeed, it was recently demonstrated that phosphorylation of voltage-gated sodium channel modulates arrhythmia and cardiac function [9], suggesting that changes in the electrical activity of myocardial cells after myocardial infarction might be the basis for arrhythmia [10]. In addition, the activation of endocrine and paracrine function in cardiac insufficiency not only participates in left ventricular remodeling, but also promotes arrhythmia [11, 12]. Despite these interesting findings, the exact role of ventricular remodeling in arrhythmia development after myocardial infarction remains unclear. Therefore, we aimed in this study to explore the relationship between ventricular remodeling and cardiac electrophysiological changes after myocardial infarction *in vivo* and *in vitro*. We found a linear relationship between cardiac electrophysiological parameters and cardiac structure on the one hand, and myocardial tissue fibrosis on the other hand, suggesting that prevention and treatment of ventricular remodeling plays a critical role in reducing arrhythmia after myocardial infarction.

Material and methods

Animals

Specific pathogen-free (SPF) Sprague Dawley (SD) rats (220 ± 10 g, 8 weeks old) were purchased from Vital River Experimental Animal Company (China) with License Number SCXK [Beijing] 2007-0001. Rats were fed standard rat chow *ad libitum*. This study was approved by the Ethics Committee of Experimental Animals, Dongzhimen Hospital, Beijing University of Chinese Medicine.

Reagents and instruments

Anti-type I and type III collagen antibodies (Boster Biological Engineering Co., Wuhan, China, BA0326 and BA0325, respectively), rabbit two-stage immunohistochemical kit (PV-6001, Zhongshan Golden Bridge Biotechnology Co., Ltd., Beijing, China), Ultrasonic diagnostic instrument (Philips, The Netherlands, HDI 5000), 15 MHZ high-frequency linear array probe and BL-420F biological function experiment system (Thaimeng technology co., LTD., Chengdu, China), Small animal ventilator (Kent Scientific, USA), SPOTII software V3.0 Image system (DIAGNOSTIC INSTRUMENTS co., LTD, USA), and Meta Morph Imaging System Version 4.5 image processing system (Universal Imaging Corporation, USA) were used in this study.

Establishment of the MI rat model

Models were made as the previous research described [13]. Briefly, anesthetized SD rats (intraperitoneal administration of 50 mg/kg sodium pentobarbital) were submitted to endotracheal intubation, and positive pressure ventilation was applied. Under preoperative monitoring by twelve-lead electrocardiogram (ECG), local skin was disinfected and the chest opened. This was followed by thoracotomy device setup and opening of the pericardium. Then, occlusion of the left anterior descending coronary artery was carried out between the pulmonary cone and the left atrial appendage under its origin 2-3 mm. Successful ligation was confirmed by ST segment elevation in postoperative Electrocardiograph (ECG), compared with preoperative values. Penicillin was administered to animals post-surgery by i.p. injection for three days. Sham animals were treated similarly, but without ligation of the left coronary. All animals were conventionally maintained after surgery. Experiments were done at 8 weeks after modeling.

Echocardiography

A Philips HDI 5000 ultrasound diagnostic instrument and 15 MHZ high-frequency linear array probe were used to assess cardiac structure and function. Measurements were carried out by two-dimensional ultrasound-guided M-curve in the parasternal long axis section. Each of the indicators including interventricular septal end diastole and systole (IVSd and IVSs, mm), left ventricular posterior wall end diastole and end systole (LVPWs and LVPWd, mm), left ventricle in systole and diastole (LVs and LVd, mm), left atrial end systolic diameter (LADs, mm) was averaged after three measurements. Ejection fraction (EF) was derived as $(LVd^3-LVs^3)/LVd^3$.

Immunohistochemical staining

3-4 mm tissue blocks were collected along the cardiac maximum diameter and paraffin-embedded after fixation with 4% paraformaldehyde. Then, improved Masson staining was used to assess myocardial tissue collagen expression. The two-step-immunohistochemical method was used to evaluate the expression of types I and III collagen. Images were acquired using the SPOTII software V3.0 on Image capture system in five high power fields of non-infarcted areas, and analyzed by Meta Morph Imaging System Version 4.5 image analysis software.

Ventricular fibrillation induced by electrical stimulation in vivo

The experiments were carried out as described previously [14]. Briefly, rats were anaesthetized by i.p. injection of 50 mg/kg sodium pentobarbital, and connected to the BL-420F biological function experimental system. The pericardium was torn after opening of the chest, and two stimulating electrodes were hooked to the left ventricular apex (positive) and left ventricular anterior infarct zone (negative). The depth of hooking was about 1 mm and the two electrodes were separated by about 3 mm with programmable serial stimulus. Each string began at 10 stimulus wave, with a pulse width of 5 ms from 1 V stimulus increased every 30 s by 1 V to the final value of 20 V.

The ventricular fibrillation threshold caused by electrical stimulation was measured. The durations of ventricular fibrillation in both groups were compared at four stages, including 1-5 V, 6-10 V, 11-15 V and 16-20 V. After left ventricular stimulation, two electrodes, respectively, were placed at the right ventricular apex (anode) and right ventricular anterior wall (cathode), separated about 3 mm and triggered by right ventricular fibrillation threshold and the duration of ventricular fibrillation of both groups in the four stages with the same stimulus mode.

Electrophysiological experiments in vitro

Reverse perfused heart from the aorta was carried out by Langendorff perfusion with conventional biological technology. The Krebs-Henseleit physiological solution contained NaCl 6.92 g/L, KCl 0.35 g/L, $MgSO_4 \cdot 2H_2O$ 0.29 g/L, $CaCl_2$ 0.28 g/L, KH_2PO_4 0.16 g/L, Glucose 2.0 g/L, and $NaHCO_3$ 2.1 g/L, with the pH adjusted to 7.2-7.4. A gas mixture (95% O_2 and 5% CO_2) was used to maintain ventilation at 2 L/min during the experiment. The perfusion solution was maintained at 38°C by a constant temperature water bath pump. The electrophysiological indicators of left ventricle, right ventricle, and left atrium were recorded continuously within 15 min under fixed frequency electrical stimulation with the BL-420 biological function experiment system, including action potential duration at 20% repolarization (APD_{20}, ms), action potential duration at 50% repolarization (APD_{50}, ms), action potential duration at 90% repolarization (APD_{90}, ms), the most significant action potential (APA, mv), the maximum increase in zero-phase velocity (Vmax, v/s), and effective refractory period (ERP, ms). Final values were obtained by averaging eight continuous measurements.

Statistical analysis

Data are mean ± standard deviation (SD). Group t test was used for normally distributed data; otherwise, Mann-Whitney U test was employed. Multiple linear regression was used with left ventricular ERP/APD_{90} ratios as dependent variables; LAD, IVSs, IVSd, LVs, LVd, PWd, and PWs (cardiac structure), and type I collagen, type III collagen, and type III to I collagen ratio (myocardial tissue fibrosis) were independent variables. The regressive method was employed with introduction and elimination standards $P<0.05$ and $P>0.10$, respectively. Regression equations were determined solely for group values with statistically significant differences ($P<0.05$). Electrophysiology data in the sham group were considered to be normal, and the direction of gap between the model and sham groups was taken as reference. The statistical analysis was carried out with the SPSS 13.0 software (SPSS, USA).

Results

Changes of cardiac structure and function

Compared with sham animals, IVSd and IVSs in the model group were significantly reduced, with 0.72 ± 0.12 vs. 2.03 ± 0.10 mm and 0.80 ± 0.09 vs. 2.88 ± 0.50 mm, respectively (all $P<0.01$); meanwhile, LVDd and LVDs increased significantly, with 10.23 ± 0.45 vs. 4.68 ± 0.49

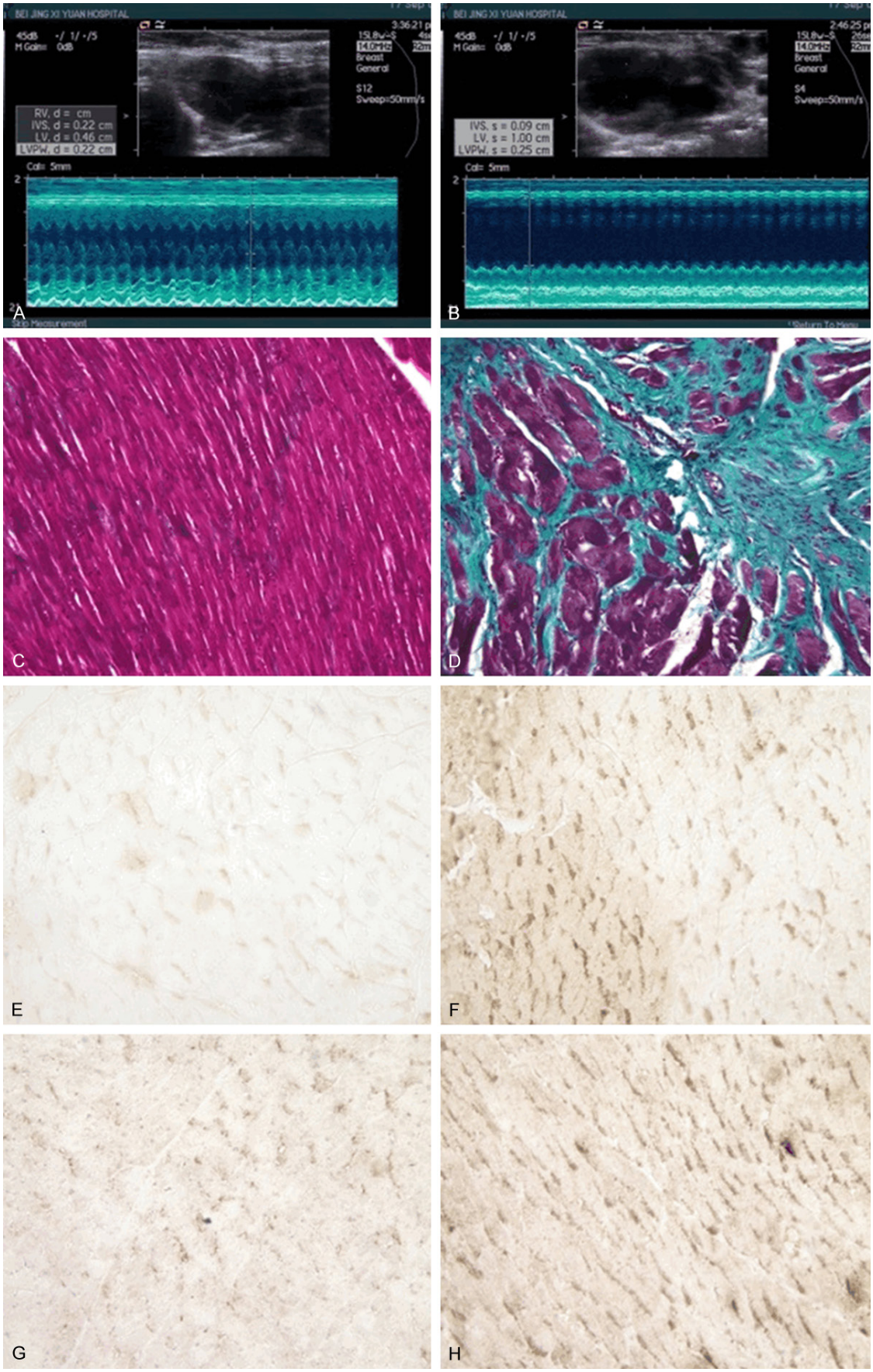
A
B
C
D
E
F
G
H

Figure 1. Morphological and collagen level changes after myocardial infarction. Representative echocardiographic images of sham (A) and model (B) rats at 8 weeks after MI acquired on an ultrasound diagnostic instrument (Philips, HDI 5000) and 15 MHZ high-frequency linear array probe; Masson staining of samples from sham (C) and model (D) animals (×200); type I collagen levels at the infarction border in samples from the sham (E) and model (F) groups detected by immunohistochemistry (×400); type III collagen at the infarction border in samples from the sham (G) and model (H) groups assessed by immunohistochemistry (×400).

mm and 9.12 ± 0.63 vs. 2.50 ± 0.50 mm, respectively (all $P<0.01$). Ejection fractions (EFs) were reduced significantly in model animals (25.07 ± 3.20%) compared with the control group (82.37 ± 8.83%, $P<0.01$). However, LADs, LVPWd and LVPWs showed similar values in both groups ($P>0.05$). Compared with the sham group, myocardial collagen volumes in model animals were increased significantly, with 15688.83 ± 2049.96 vs. 2158.11 ± 169.09 μm^2 ($P<0.01$). In addition, types I and III collagen amounts were markedly increased, with 13698.17 ± 2223.19 vs. 1775.47 ± 300.92 μm^2 and 1535.17 ± 102.42 vs. 356.88 ± 16.64 μm^2, respectively (all $P<0.01$); meanwhile, type III/I collagen ratios decreased significantly (11.51-2.29 vs. 20.63 + 3.95, $P<0.01$) as shown in **Figure 1**.

Ventricular fibrillation threshold and duration are altered by electrical stimulation

The left and right ventricles in model rats were stimulated by programmed electrical stimulation at 8 weeks after MI. Ventricular fibrillation thresholds of rats in the model group were decreased significantly compared with those obtained for sham animals ($P<0.01$); in addition, ventricular fibrillation durations induced by left and right ventricular electrical stimulations were prolonged significantly ($P<0.01$, $P<0.05$) as assessed by Mann-Whitney U test (**Figure 2**).

Changes of cardiac electrophysiological parameters after AMI

Compared with sham rats, APD_{20}, APD_{50} and APD_{90} of left and right ventricles in rats of the model group were markedly prolonged (all $P<0.01$), while APA and Vmax showed no significant differences (all $P>0.05$). In addition, APD_{50} and APD_{90} of left atrium were prolonged significantly ($P<0.01$ and $P<0.05$, respectively); however, APD_{20}, APA and Vmax were similar between both groups ($P>0.05$). The discrete degrees of APD_{90} in left ventricle-left atrium and right ventricle-left atrium obviously increased ($P<0.01$) in the model group compared with sham animals; ERP values for left and right ventricles significantly increased as well ($P<0.01$). ERP/APD_{90} ratios of left and right ventricles both significantly decreased ($P<0.01$), while the discrete degree of ERP in left ventricle-right ventricle increased significantly in the model group compared with controls ($P<0.05$, **Figure 3**).

Association of cardiac electrophysiological parameters and heart structure

The LAD, IVSd, LVd, PWd, IVSs, LVs and PWs values (obtained by ultrasound) and ventricular fibrillation threshold were analyzed in multiple stepwise regression. A total of 7 regression equations were obtained. The final regression equation was determined by combination of medical analysis and statistics: $y=1.34 + 4.12x$ ($P<0.01$, $R=0.61$) where x represents IVSd, and y ventricular fibrillation threshold (VFT); this was the optimal regression equation according to medical logic and statistical principles.

The left ventricle ERP/APD_{90} ratios in the model and sham groups, left ventricular wall thicknesses, and left ventricular cavity areas were analyzed in multiple stepwise regression at eight weeks after modeling, with LAD, IVSd, LVd, PWd, IVSs, LVs, and PWs detected by ultrasound. A total of 7 regression equations were derived and the final regression equation was determined as: $y=0.75-0.026x$ ($P<0.01$, $R=0.94$), where x is LVs, and y the left ventricular ERP/APD_{90} ratio; this was the optimal regression equation.

Association of cardiac electrophysiological parameters and myocardial tissue fibrosis

The total collagen level in left ventricle, type I and III collagen amounts, and type III/I collagen ratio obtained by pathological dyeing and ventricular fibrillation threshold were analyzed in multiple stepwise regression. A total of 4 regression equations were obtained and the final regression equation was determined as: $y=11.30-0.005x$ ($P<0.01$, $R=0.59$), where x is

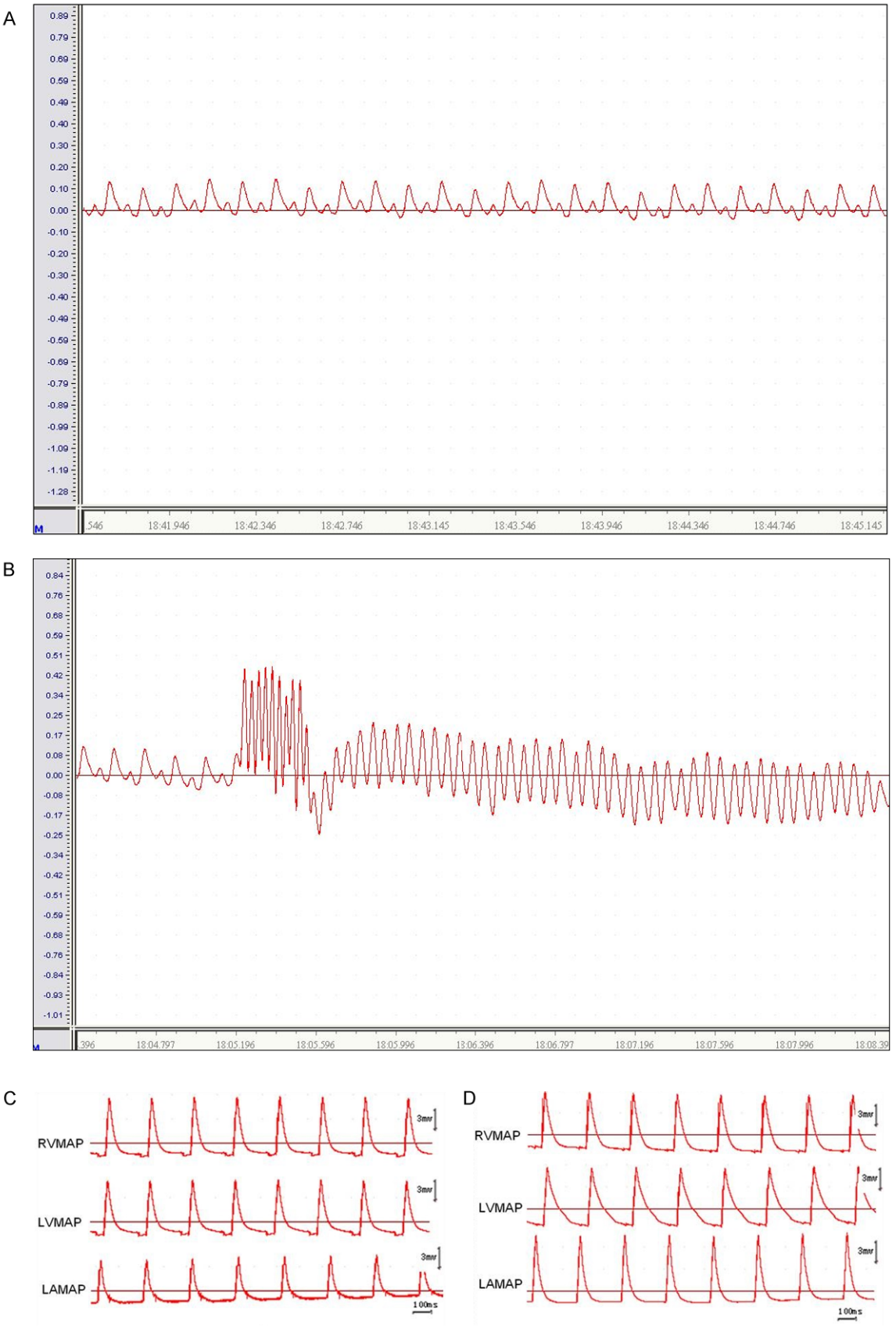
A
B
C
RVMAP
LVMAP
LAMAP
3mv
100ms
D
RVMAP
LVMAP
LAMAP
3mv
100ms

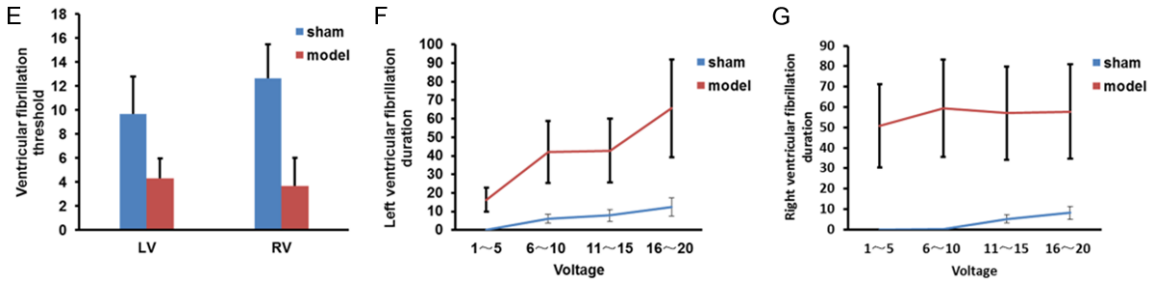

Figure 2. Changes of ventricular fibrillation threshold and duration after electrical stimulation. A. II lead ECG data of sham animals before thoracotomy (HR: 400/min, maximum voltage: 0.15 mv, minimum voltage: -0.01 mv, volt top-top value: 0.14 mv). B. II lead ECG of ventricular fibrillation caused by the electrical stimulation, after thoracotomy in the model group (HR: 900/min, maximum voltage: 0.45 mv, minimum voltage: -0.25 mv, volt top-top value: 0.70 mv). C. Monophasic action potential in sham animals *in vitro*: RVMAP, LVMAP and LAMAP are monophasic action potentials of right ventricle, left ventricle and left atrium, respectively. D. Monophasic action potential in model rats *in vitro*: RVMAP, LVMAP and LAMAP are monophasic action potentials of right ventricle, left ventricle and left atrium, respectively. E. Thresholds of left and right ventricular fibrillation. F. Duration of left ventricular fibrillation. G. Duration of right ventricular fibrillation. **P*<0.05, ***P*<0.01 vs. sham.

type III collagen level, and y ventricular fibrillation threshold; this was the optimal regression equation.

The left ventricle ERP/APD_{90} ratios were analyzed in multiple stepwise regression with the total collagen level in left ventricle, type I and III collagen amounts, and type III/I collagen ratios. A total of 4 regression equations were obtained and the final regression equation was determined as: $y=0.71-137.37x_1 + 0.002x_2$ (*P*<0.01, R=0.90), where x_1 is type III collagen level, x_2 is type III/I collagen ratio, and y the left ventricle ERP/APD_{90} ratio; this was the optimal regression equation.

Discussion

In this study, we found reduced IVSd, IVSs, type III/I collagen ratios, and VFT values in the model group compared with sham rats at 8 weeks after modeling, meanwhile, LVDd, LVDs, total myocardial collagen, and type I and III collagen contents significantly increased. In addition, left and right ventricular ERP/APD_{90} ratios decreased significantly. Furthermore, a linear relationship was obtained between cardiac electrophysiological parameters and cardiac structure on the one hand and myocardial tissue fibrosis on the other hand.

Left ventricular volumes in model rats were increased at 8 weeks with ventricular wall thickness remaining unchanged; collagen levels were enhanced, and the left ventricle showed a concentric hypertrophy. Left ventricular remodeling after myocardial infarction resulted in significantly reduced fibrillation threshold and prolonged ventricular fibrillation, with the organ more prone to malignant arrhythmia. Continuous development of left ventricular remodeling after myocardial infarction also gradually initiated or aggravated right ventricular remodeling, causing a decline of right ventricular fibrillation threshold triggered by electrical stimulation in the late-phase of myocardial infarction as well as changes of electrophysiological characteristics, further illustrating the effect of cardiac remodeling on electrophysiological properties.

Monophasic action potential is a reliable index for the myocardial bipolar process [15]. Length of ventricular muscle action potential (APD) mainly depends on repolarization speed. Action potential duration at 50% repolarization is termed APD_{50}, and mainly reflects the ventricular effective refractory period (ERP). In general, ERP and APD change in the same direction, and increased ERP/APD ratios have an anti-arrhythmia effect [16]. Ventricular fibrillation threshold is an important index that reflects the cardiac electrical stability and ease of ventricular fibrillation. VFT significantly decreases in heart failure, favoring malignant ventricular arrhythmia as a result of ventricular electrical instability caused by various reasons [17].

In vitro assessment of cardiac electrophysiology showed significantly extended APD_{20}, APD_{50} and APD_{90} of left and right ventricles in the model group at 8 weeks after myocardial infarc-

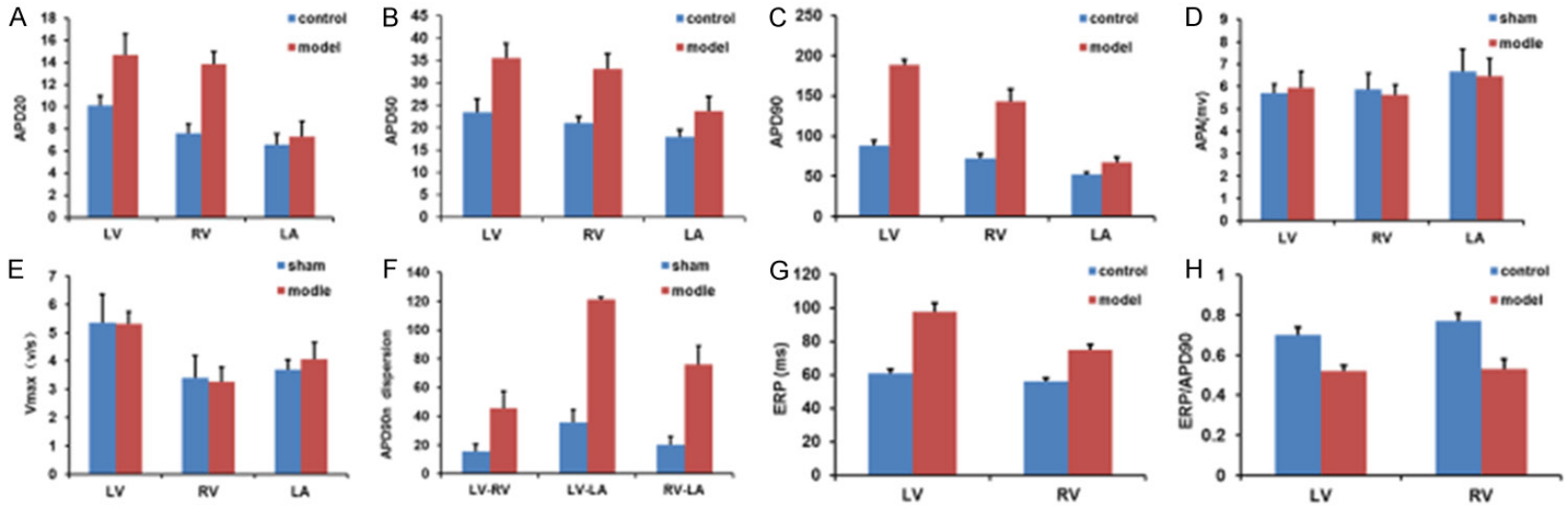

Figure 3. Changes of cardiac electrophysiological parameters after AMI *in vivo*. A. APD_{20}, B. APD_{50}, C. APD_{90}, D. APA, E. Vmax, F. APD_{90} dispersion degree, G. ERP, H. ERP/APD_{90} ratios. **P*<0.05, ***P*<0.01 vs. sham.

tion, as shown above. The prolonged ventricular action potential after myocardial infarction is consistent with previous findings [18]. We also demonstrated that despite significantly prolonged left and right ventricular myocardial APD and ERP in rats after ventricular remodeling, ERP/APD_{90} ratios decreased, while the discrete degrees of APD_{90} and ERP increased. When the myocardial action potential generated by electrical excitation falls out of the effective and relative refractory periods, abnormal electrical impulses and anisotropic conduction are easily generated, leading to the excitement of more ectopic rhythms and exhumation formation, which may be one of the electrophysiological mechanisms by which ventricular remodeling causes arrhythmia.

By multiple regression analysis we found a positive correlation between ventricular fibrillation threshold after AMI and the parameters of left ventricular wall thickness IVSd, IVSs and PWd. In addition, ERP/APD_{90} ratio, which is important for electrical stability, was positively correlated with the parameters of left ventricular wall thickness such as IVSs and PWs. The heart of rats with myocardial infarction had concentric hypertrophy because concentric remodeling leads to the interventricular septum and left ventricular posterior wall thinning. The thinner the left ventricular wall, the lower the ventricular fibrillation threshold, so is the ERP/APD_{90} ratio. These all lead to ventricular electrical instability, which results in electrical excitation generated by myocardial action potential falling out of effective and relative refractory periods, easing the production of abnormal electrical impulses and anisotropic conduction; this in turn leads to the excitement of more ectopic rhythms as well as the formation of large, small and micro turn-back loops, making ventricular fibrillation easier.

Types I and III collagen were predominantly in the myocardium. Type I collagen has limited elasticity, pronounced stiffness and strong resistance in maintaining ventricular wall strength, polymerizing into a fiber net. Type III Collagen has extended resilience, with fine and very elastic fibers; it is associated with ventricular wall elasticity, forming the fine fiber net. After myocardial infarction rats showed myocardial fiber hyperplasia to different degrees, caused by changes in types I and III collagen levels, with increased type I collagen level as the major factor. And increased myocardial fibrosis degree can lead to cardiac arrhythmia. The possible mechanism is that fibrosis between myocardial and myofibers could increase electrical anisotropy, and cause some electric coupling loss, eventually increasing the coupling impedance between myocardial cells [19]. In this case, impulse transmission does not occur in the direction of normal cell coupling, thus blocking impulse conduction and exhumation formation [20, 21]; loss of cell coupling may cause decreased cell bipolar space, which in turn, leads to directional block and exhumation.

Therefore, myocardial fiber hyperplasia in the heart with ventricular remodeling after myocardial infarction is an important mechanism behind cardiac arrhythmias caused by ventricular remodeling. Multivariate regression analysis showed that VFT and ERP/APD_{90} ratio were inversely proportional to type III collagen levels. The worse the ventricular remodeling after myocardial infarction, the more pronounced the type III collagen hyperplasia and the lower the ERP/APD_{90} ratio, illustrates that ventricular remodeling not only leads to cardiac function decompensation, but also causes cardiac arrhythmias (even malignant arrhythmia).

In conclusion, the relationships between cardiac structure in rats and pathological and physiological functions were qualitatively and quantitatively analyzed. This was done through the assessment of organ and tissue pathomorphological changes during ventricular remodeling after myocardial infarction as well as multiple regression analysis of ventricular fibrillation and ERP/APD_{90} ratio. Ventricular remodeling not only leads to cardiac function decompensation, but also causes cardiac arrhythmias. Therefore, prevention and treatment of ventricular remodeling after myocardial infarction is crucialin reducing arrhythmia occurrence in patients with myocardial infarction (MI). Clinical application of ACEI, ARB, beta blockers and other drugs can inhibit the ventricular remodeling and reduce ventricular arrhythmia occurrence. A deep understanding of the relationship between ventricular remodeling and cardiac electrophysiology is critical for the development of new anti-arrhythmic therapy and screening of high-risk groups, providing a fundamental basis for arrhythmia prevention and control.

Acknowledgements

This paper was supported by the National Science Foundation Project of China (No. 30672754, 81473662).

Disclosure of conflict of interest

None.

Address correspondence to: Shuoren Wang, Key Laboratory of Chinese Internal Medicine (Beijing University of Chinese Medicine), Ministry of Education, Dongzhimen Hospital, Beijing University of Chinese Medicine, Beijing 100700, China. Tel: +86-13121306161; Fax: +86-010-84013229; E-mail: chaweto@126.com

References

[1] Sicouri S and Antzelevitch C. A subpopulation of cells with unique electrophysiological properties in the deep subepicardium of the canine ventricle. The M cell. Circ Res 1991; 68: 1729-1741.

[2] Antzelevitch C, Sun ZQ, Zhang ZQ and Yan GX. Cellular and ionic mechanisms underlying erythromycin-induced long QT intervals and torsade de pointes. J Am Coll Cardiol 1996; 28: 1836-1848.

[3] Jones JR, Mata JF, Yang Z, French BA and Oshinski JN. Left ventricular remodeling subsequent to reperfused myocardial infarction: evaluation of a rat model using cardiac magnetic resonance imaging. J Cardiovasc Magn Reson 2002; 4: 317-326.

[4] St John Sutton M, Lee D, Rouleau JL, Goldman S, Plappert T, Braunwald E and Pfeffer MA. Left ventricular remodeling and ventricular arrhythmias after myocardial infarction. Circulation 2003; 107: 2577-2582.

[5] Swynghedauw B. Molecular mechanisms of myocardial remodeling. Physiol Rev 1999; 79: 215-262.

[6] Draper TS Jr, Silver JS and Gaasch WH. Adverse structural remodeling of the left ventricle and ventricular arrhythmias in patients with depressed ejection fraction. J Card Fail 2015; 21: 97-102.

[7] Huang B, Qin D and El-Sherif N. Spatial alterations of Kv channels expression and K(+) currents in post-MI remodeled rat heart. Cardiovasc Res 2001; 52: 246-254.

[8] Sasano T, McDonald AD, Kikuchi K and Donahue JK. Molecular ablation of ventricular tachycardia after myocardial infarction. Nat Med 2006; 12: 1256-1258.

[9] Glynn P, Musa H, Wu X, Unudurthi SD, Little S, Qian L, Wright PJ, Radwanski PB, Gyorke S, Mohler PJ and Hund TJ. Voltage-Gated Sodium Channel Phosphorylation at Ser571 Regulates Late Current, Arrhythmia, and Cardiac Function In Vivo. Circulation 2015; 132: 567-577.

[10] Aimond F, Alvarez JL, Rauzier JM, Lorente P and Vassort G. Ionic basis of ventricular arrhythmias in remodeled rat heart during long-term myocardial infarction. Cardiovasc Res 1999; 42: 402-415.

[11] Golden KL, Ren J, Dean A and Marsh JD. Norepinephrine regulates the in vivo expression of the L-type calcium channel. Mol Cell Biochem 2002; 236: 107-114.

[12] Marx SO, Kurokawa J, Reiken S, Motoike H, D'Armiento J, Marks AR and Kass RS. Requirement of a macromolecular signaling complex for beta adrenergic receptor modulation of the KCNQ1-KCNE1 potassium channel. Science 2002; 295: 496-499.

[13] Wu A, Zhai J, Zhang D, Lou L, Zhu H, Gao Y, Chai L, Xing Y, Lv X, Zhu L, Zhao M and Wang S. Effect of wenxin granule on ventricular remodeling and myocardial apoptosis in rats with myocardial infarction. Evid Based Complement Alternat Med 2013; 2013: 967986.

[14] Jiao KL, Li YG, Zhang PP, Chen RH and Yu Y. Effects of valsartan on ventricular arrhythmia induced by programmed electrical stimulation in rats with myocardial infarction. J Cell Mol Med 2012; 16: 1342-1351.

[15] Franz MR. Long-term recording of monophasic action potentials from human endocardium. Am J Cardiol 1983; 51: 1629-1634.

[16] Hohnloser SH and Singh BN. Proarrhythmia with class III antiarrhythmic drugs: definition, electrophysiologic mechanisms, incidence, predisposing factors, and clinical implications. J Cardiovasc Electrophysiol 1995; 6: 920-936.

[17] Cittadini A, Monti MG, Isgaard J, Casaburi C, Stromer H, Di Gianni A, Serpico R, Saldamarco L, Vanasia M and Sacca L. Aldosterone receptor blockade improves left ventricular remodeling and increases ventricular fibrillation threshold in experimental heart failure. Cardiovasc Res 2003; 58: 555-564.

[18] Perrier E, Kerfant BG, Lalevee N, Bideaux P, Rossier MF, Richard S, Gomez AM and Benitah JP. Mineralocorticoid receptor antagonism prevents the electrical remodeling that precedes cellular hypertrophy after myocardial infarction. Circulation 2004; 110: 776-783.

[19] Spach MS and Dolber PC. Relating extracellular potentials and their derivatives to anisotropic propagation at a microscopic level in human cardiac muscle. Evidence for electrical uncoupling of side-to-side fiber connections with increasing age. Circ Res 1986; 58: 356-371.

[20] Delgado C, Steinhaus B, Delmar M, Chialvo DR and Jalife J. Directional differences in excitability and margin of safety for propagation in sheep ventricular epicardial muscle. Circ Res 1990; 67: 97-110.

[21] Delmar M, Michaels DC, Johnson T and Jalife J. Effects of increasing intercellular resistance on transverse and longitudinal propagation in sheep epicardial muscle. Circ Res 1987; 60: 780-785.